JOC*Article*

Is There Stereoselectivity in Spin Trapping Superoxide by 5-*tert*-Butoxycarbonyl-5-methyl-1-pyrroline *N*-Oxide?

Pei Tsai,[†,‡] Jeffrey M. Marra,[§] Sovitj Pou,[‡] Michael K. Bowman,[∥] and Gerald M. Rosen*[,†,‡]

Department of Pharmaceutical Sciences, University of Maryland School of Pharmacy, Baltimore, Maryland 21201, Medical Biotechnology Center, University of Maryland Biotechnology Institute, Baltimore, Maryland 21201, Center for Low-Frequency EPR Imaging for In Vivo Physiology, University of Maryland, Baltimore, Baltimore, Maryland 21201, Purdue Pharma, LP, Computational, Combinatorial and Medicinal Chemistry, Cranbury, New Jersey 08512, and Structural Biology and Microimaging, Battelle Northwest, Richland, Washington 99352

Received April 7, 2005

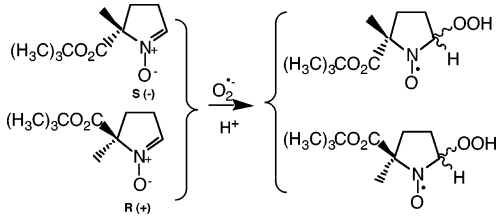

Ester-containing nitrones, including 5-*tert*-butoxycarbonyl-5-methyl-1-pyrroline *N*-oxide **5**, have been reported to be robust spin traps for superoxide ($O_2^{\bullet-}$). Using a chiral column, we have been able to isolate the two enantiomers of nitrone **5**. With enantiomerically pure nitrone **5a** and **5b** we explored whether one of these isomers was solely responsible for the EPR spectrum of aminoxyl **6**. Data obtained demonstrate that the spin trapping of $O_2^{\bullet-}$ by nitrone **5a** and nitrone **5b** affords the identical EPR spectra and lifetimes in homogeneous aqueous solution and exhibits the same ratio of *cis* and *trans* isomers. Quantum chemical modeling in vacuo also finds no difference, aside from the expected optical activity, arising from the difference in stereochemistry.

Introduction

Since the development of spin trapping in the late 1960s,[1] this technique has been the primary method to characterize free radicals generated in biological systems. For instance, spin trapping was instrumental in the discovery that nitric oxide synthase (NOS; EC 1.14.13.39), independent of the isozyme, generates superoxide ($O_2^{\bullet-}$) along with nitric oxide ($^{\bullet}NO$).[2]

The nitrone 5,5-dimethyl-1-pyrroline *N*-oxide **1** (Scheme 1) has been the primary spin trap for $O_2^{\bullet-}$, owing this standing to the unique EPR spectrum of 2-hydroperoxy-5,5-dimethyl-1-pyrrolindinyloxyl **2**,[3] despite the slow reaction rate of **1** with $O_2^{\bullet-}$ and the short lifetime of **2**. Over the past several decades, structurally diverse nitrones have been synthesized and their reactions with $O_2^{\bullet-}$ have been defined.[4] Of those nitrones, 5-(diethoxyphosphoryl)-5-methyl-1-pyrroline *N*-oxide **3** appears to be

SCHEME 1

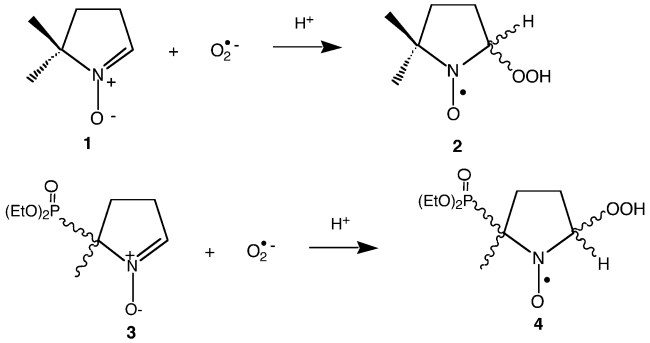

* To whom correspondence should be addressed. Tel: 410-706-0514. Fax: 410-706-8184. Email: grosen@umaryland.edu.
† University of Maryland School of Pharmacy and University of Maryland Biotechnology Institute.
‡ University of Maryland.
§ Purdue Pharma, LP.
∥ Battelle Northwest.

(1) (a) Mackor, A.; Wajer, Th. A. J. W.; de Boer, Th. J. *Tetraheron Lett.* **1966**, 2115−2123. (b) Iwamura, M.; Inamoto, N. *Bull. Chem. Soc. Jpn.* **1967**, *40*, 702. (c) Chalfont, G. R.; Perkins, M. J.; Horsfield, A. *J. Am. Chem. Soc.* **1968**, *90*, 7141−7142. (d) Janzen, E. G.; Blackburn, B. J. *J. Am. Chem. Soc.* **1968**, *90*, 5909−5910. (e) Lagerscrantz, C.; Forshult, S. *Nature* **1968**, *218*, 1247−1248.

(2) (a) Pou, S.; Pou, W. S.; Bredt, D. S.; Snyder, S. H.; Rosen, G. M. *J. Biol. Chem.* **1992**, *267*, 24173−24176. (b) Xia, Y.; Roman, L. J.; Masters, B. S.; Zweier, J. L. *J. Biol. Chem.* **1998**, *273*, 22635−22639. (c) Vasquez-Vivar, J.; Kalyanaraman, B.; Martasek, P.; Hogg, N.; Masters, B. S.; Karoui, H.; Tordo, P.; Pritchard, K. A., Jr. *Proc. Natl. Acad. Sci. U.S.A.* **1998**, *95*, 9220−9225. (d) Xia, Y.; Tsai, A. L.; Berka, V.; Zweier, J. L. *J. Biol. Chem.* **1998**, *273*, 25804−25808. (e) Pou, S.; Keaton, L.; Surichamorn, W.; Rosen, G. M. *J. Biol. Chem.* **1999**, *274*, 9573−9580. (f) Yoneyama, H.; Yamamoto, A.; Kosaka, H. *Biochem. J.* **2001**, *360*, 247−253.

10.1021/jo050692f CCC: $30.25
Published on Web 08/09/2005

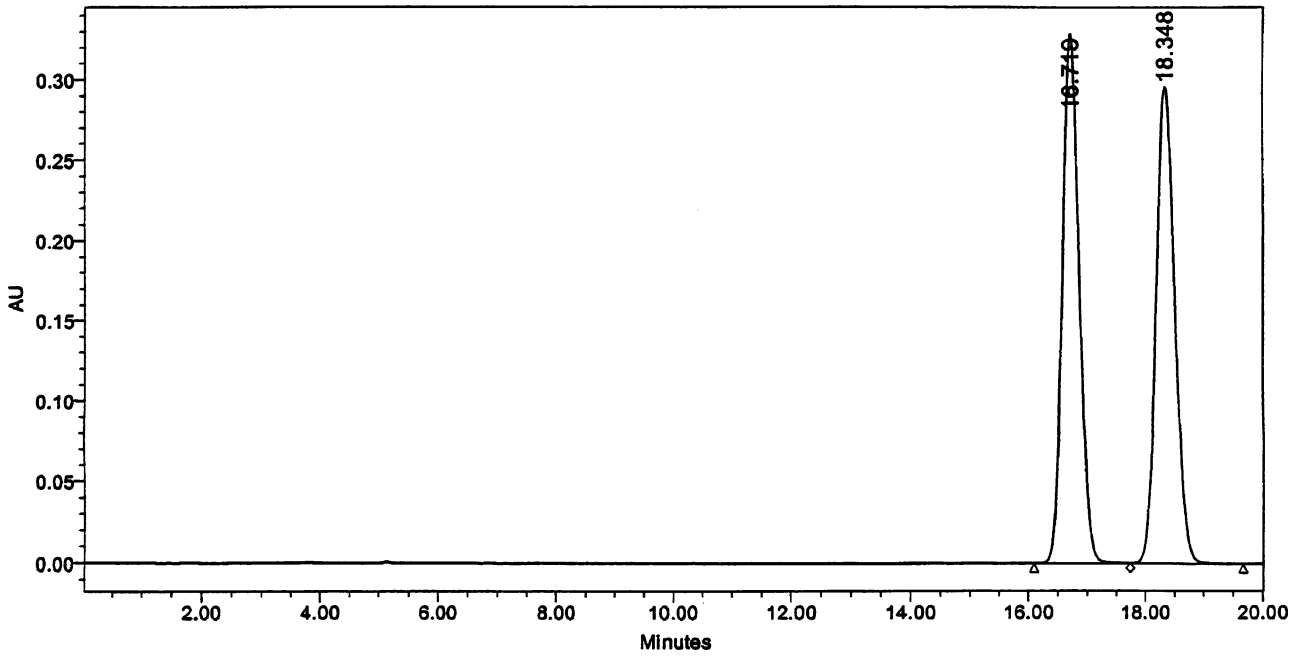

FIGURE 1. Representative HPLC scan of the separation of the racemate of 5-*tert*-butoxycarbonyl-5-methyl-1-pyrroline *N*-oxide into the two isomers. The first peak is **5a**, the *S*(−) enantiomer, and the second peak is **5b**, the R(+) enantiomer (Scheme 2). See Experimental Section for more details.

one of the most promising compounds (Scheme 1).[5] Alternative probes for $O_2^{\bullet-}$, however, include a family of ester-containing nitrones, first synthesized in 1959[6] and currently reported to be robust spin traps for this free radical.[7] The corresponding aminoxyls exhibit EPR spectra similar to those ascribed to aminoxyl **2**. Soon thereafter, on the basis of experimental data and quantum mechanical and EPR spectral modeling, we suggested that the recorded EPR spectrum of aminoxyl **2** is a composite of two conformers, with a distribution of 54% and 46%.[8] Similarly, the EPR spectrum of aminoxyl **6**, for instance, derived from the reaction of 5-*tert*-butoxycarbonyl-5-methyl-1-pyrroline *N*-oxide **5** with $O_2^{\bullet-}$, is

SCHEME 2

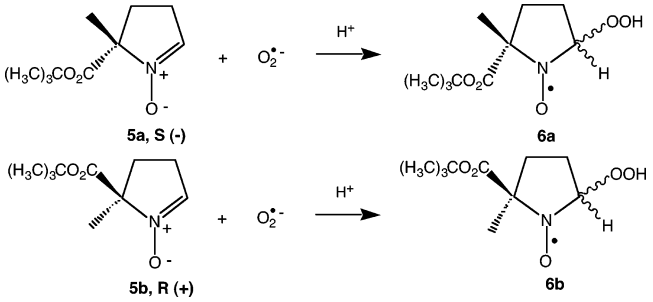

nearly identical to that of aminoxyl **2**,[7e,8] and as in the case of aminoxyl **2**, the EPR spectrum of **6** appears to be composed of two conformers, with a distribution of 59% and 41%.[7e] Given that nitrone **5** is a racemic mixture (Scheme 2), we decided to explore whether one of the enantiomers was solely responsible for the EPR spectrum of aminoxyls **6a** and **6b**, which are each a mixture of two diasteromers *trans* and *cis* with respect to the ester at position 5.

Results and Discussion

Initially we sought an HPLC method that would separate nitrones **5a** and **5b**. After a series of pilot experiments, we settled on a ChiralPak AD H column, eluting with hexanes/ethanol/methanol/diethylamine (95: 2.5:2.4:0.1). A representative trace is shown in Figure 1**.**

With enantiomerically pure **5a** and **5b** in hand, we turned our attention to the assignment of the absolute stereochemistry by analogy to known compounds. We included *N*-carboxyl-substituted prolines as models, because optical rotation is essentially due to anisotropic polarization of the molecule, which is related to the dipole moment. We believe that the overall dipole of the

(3) (a) Harbour, J. R.; Chow, V.; Bolton, J. R. *Can. J. Chem.* **1974**, *52*, 3549−3553. (b) Finkelstein, E.; Rosen, G. M.; Rauckman, E. J. *Mol. Pharmacol.* **1979**, *16*, 676−685. (c) Kalyanaraman, B.; Perez-Reyes, E.; Mason, R. P. *Biochim. Biophys. Acta* **1980**, *630*, 119−130. (d) Mottley, C.; Connor, H. D.; Mason, R. P. *Biochem. Biophys. Res. Commun.* **1986**, *141*, 622−628.

(4) Rosen, G. M.; Britigan, B. E.; Halpern, H. J.; Pou, S. *Free Radicals. Biology and Detection by Spin Trapping*; Oxford University Press: New York, 1999; pp 187−273.

(5) (a) Fréjaville, C.; Karoui, H.; Tuccio, B.; Le Moigne, F.; Culcasi, M.; Pietri, S.; Lauricella, R.; Tordo, P. *J. Chem. Soc. Chem. Commun.* **1994**, 1793−1794. (b) Frejaville, C.; Karoui, H.; Tuccio, B.; Le Moigne; F., Culcasi; M., Pietri, S.; Lauricella, R.; Tordo, P. *J.* Med. Chem. **1995**, *38*, 258−265.

(6) Bonnett, R.; Brown, R. F. C.; Clark, V. M.; Sutherland, I. O.; Todd, A. *J. Chem. Soc.* **1959**, 2094−2102.

(7) (a) Olive, G.; Mercier, A.; Le Moigne, F.; Rockenbaur, A.; Tordo, P. *Free Radical Biol. Med*. **2000**, *28*, 403−408. (b) Zhang, H.; Joseph, J.; Vasquez-Vivar, J.; Karoui, H.; Nsanzumuhire, C.; Martásek, P.; Tordo, P. Kalyanaraman, B. *FEBS Lett.* **2000**, *473*, 58−62. (c) Zhao, H.; Joseph, J.; Zhang, H.; Karoui, H.; Kalyanaraman, B. *Free Radical Biol. Med.* **2001**, *31*, 599−606. (d) Stolze, K.; Udilova, N.; Rosenau, T.; Hofinger, A.; Nohl, H. *Biol. Chem.* **2003**, 384, 493−500. (e) Tsai, P.; Ichikawa, K.; Mailer, C.; Pou, S.; Halpern, H. J.; Robinson, B. H.; Nielsen, R.; Rosen, G. M. *J. Org. Chem.* **2003**, *68*, 7811−7817. (f) Weaver, J.; Tsai, P.; Pou, S.; Rosen, G. M. *J. Org. Chem*. **2004**, *69*, 8423−8428.

(8) Rosen, G. M.; Beselman, A.; Tsai, P.; Pou, S.; Mailer, C.; Ichikawa, K.; Robinson, B. H.; Nielsen, R.; Halpern, H. J.; MacKerell, A. D., Jr. *J. Org. Chem.* **2004**, *69*, 1321−1330.

N-formyl and *N*-BOC prolines is more similar to that of **5a** and **5b** than proline, per se. We have included the rotations of L-proline and L-proline *tert*-butyl ester to show that the nature of the ester does not alter the direction of rotation, and the rotation of *N*-formyl L-proline *tert*-butyl ester is included to show that the shift in the dipole also does not alter the direction of rotation. There is literature precedent for the α-alkyl nature of the molecule to invert the rotation from levorotatory to dextrorotatory;[9a,9b] therefore we have used only α-methyl compounds for comparison where data were available. The standard rotation for α-methyl-L-proline is −71,[9c] and that for *N*-BOC α-methyl-L-proline is −41.4.[9a] The standard rotation for L-proline is −84, that for the *tert*-butyl ester of L-proline is −41.5, and that for the *N*-formyl *tert*-butyl ester of L-proline is −109.8.[9d] Natural L-proline is in the *S* configuration, and all related examples conserve the negative sign of rotation. The first peak eluted had negative rotation; therefore, on the basis of data presented above, we propose that **5a** is the *S*(−) enantiomer and **5b** is the *R*(+) enantiomer.

Given that we have isolated and purified the two isomers of nitrone **5**, three questions immediately come to mind. First, will nitrone **5a** and nitrone **5b** spin trap $O_2^{\bullet-}$? Second, if each isomer reacts with $O_2^{\bullet-}$, is there a difference in the rate constant for this reaction? Third, even though both enantiomers of nitrone **5** react with $O_2^{\bullet-}$, are the stabilities of aminoxyl **6a** and aminoxyl **6b** disparate?

In the next series of experiments, we incubated either enantiomer nitrone **5a**, nitrone **5b**, or the racemate of nitrone **5** with the $O_2^{\bullet-}$ generating system, consisting of hypoxanthine/xanthine oxidase. The initial rate of $O_2^{\bullet-}$ production was 1 μM/min. The EPR spectrum of aminoxyl **6** is composed of two sets of diastereomers with A_N = 13.22 G, A_H^{β} = 11.77 G for one set of diastereomers and A_N = 13.21 G, A_H^{β} = 9.47 G for the other (Figure 2A). Under identical conditions, enantiomer nitrone **5a** and nitrone **5b** gave the same EPR spectrum as the racemate did, even equivalent ratios of diastereomers at 59% and 41%, respectively (Figure 2C and B).

The next series of experiments were devoted to determining the rate constant for the reaction of $O_2^{\bullet-}$ with each isomer and the racemate. The competitive kinetic model previously described[9] using SOD as the competitive inhibitor was employed for these studies.[7f] We found that the apparent rate constant for each isomer was the same, $k \approx 70\ M^{-1}\ s^{-1}$, with no difference from that reported for the racemate nitrone **5**.[7f] Similarly, the half-life for aminoxyls **6a** and **6b**, was determined to be ∼20 min., equivalent to that measured for aminoxyl **6**, derived from the racemate nitrone **5**.[7e]

Optimization of the *trans* aminoxyl with the hydroperoxyl and ester groups on opposite faces of the pyrroline ring using density functional theory (DFT) converged to the same two local energy minima for either **6a** or **6b** with the structures shown in Figure 3. Both structures feature an internal hydrogen bond between the oxygen

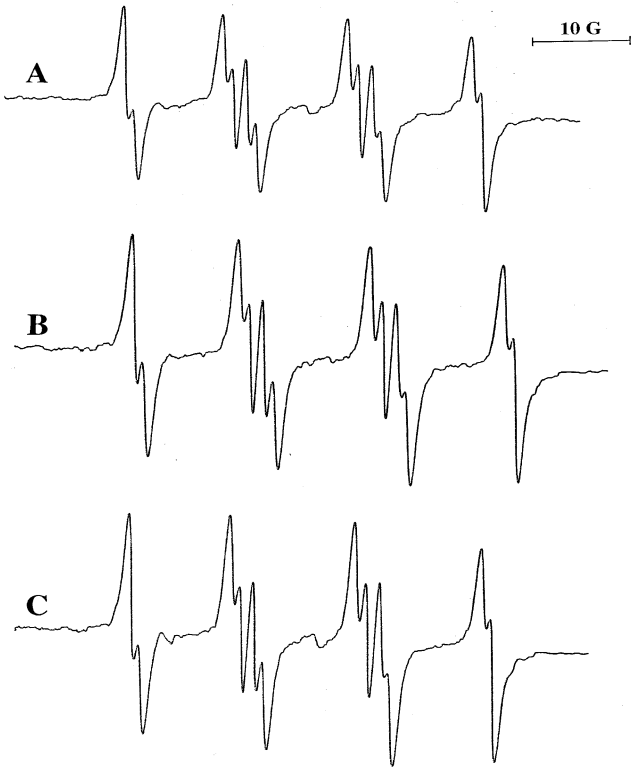

FIGURE 2. EPR spectra, derived from the reaction of nitrone **5** with $O_2^{\bullet-}$ using hypoxanthine/xanthine oxidase reaction system. The reaction mixture contained nitrone **5** (50 mM), hypoxanthine (400 μM), and sufficient xanthine oxidase to generate about 1.2 μM/min in potassium phosphate buffer (50 mM, pH7.0, containing 1 mM DTPA). EPR spectra were recorded at room temperature after the reaction was initiated by the addition of xanthine oxidase. Receiver gain was 2.5 × 10^4, scan speed was 12.5 G/min. (A) Racemate of nitrone **5**; (B) nitrone **5b**; (C) nitrone **5a**.

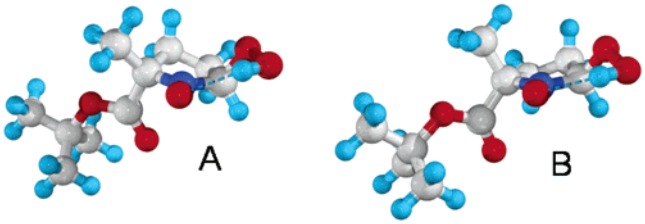

FIGURE 3. Two lowest-energy conformations of the *trans* aminoxyl **6** with the hydrogen bond indicated by the dashed line between the proton on the hydroperoxy group and the aminoxyl oxygen. (A) The most stable conformation found; (B) the next most stable conformation, 1.37 kJ/mol higher in energy.

of the aminoxyl and the hydroperoxyl group. The aminoxyl and its neighboring carbons are planar in both structures, whereas the other two carbons in the ring are twisted out of plane. The structure in Figure 3A is lower in energy by 0.327 kcal/mol from the DFT calculations. The two *trans* bulky groups, the hydroperoxyl and the ester, are both in axial positions on the pyrroline ring. The less stable conformation, Figure 3B, has the ring in the opposite twist and the bulky groups are neither axial nor equatorial. Interestingly, the internal hydrogen bond seems to be stronger, with shorter O−H distances, 2.031 versus 2.060 Å, and O−O distances, 2.805 versus 2.842

(9) (a) Beck, A. K.; Blank, S.; Job, K.; Seebach; D.; Sommerfeld, T. *Org. Synth*. **1993**, 72, 62−73. (b) Khalil, E. M.; Ojala, W. H.; Pradhan, A.; Nair, V. D.; Gleason, W. B.; Mishra, R. K.; Johnson, R. L. *J. Med Chem*. **1999**, *42*, 628−637. (c) Khalil, E. M.; Subasinghe, N. L.; Johnson, R. L. *Tetrahedron Lett*. **1996**, *37*, 3441−3444. (d) Waki, M.; Meienhofer, J. *J. Org. Chem.* **1977**, *42*, 2019−2020.

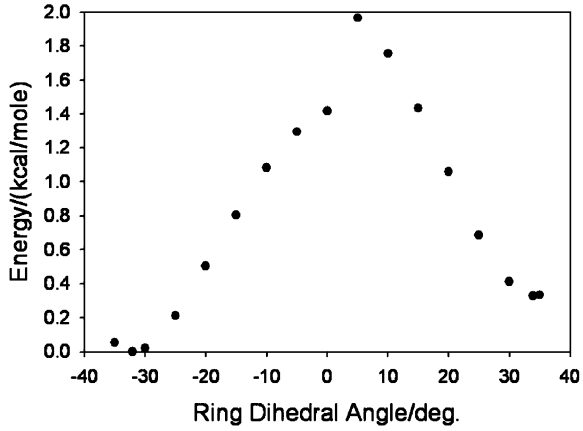

FIGURE 4. DFT energies calculated from constrained geometry optimization as a function of the dihedral angle of the C−C bond opposite the aminoxyl group in the ring of *trans* **6**. Optimizations were done in order starting from the right-hand side of the figure. The abrupt change at an angle of 0° corresponds to a jump from one energy minimum to another.

Å, compared to the more stable conformation in Figure 3A. The two structures in Figure 3A and B are similar to ring pucker 1 and 2 structures, respectively, found in aminoxyl **2**,[8] although the relative stabilities are reversed.

The energy barrier for interconversion of these two conformations was estimated by stepping the dihedral angle around the C−C bond in the ring opposite the aminoxyl group from the less stable (33.94°) toward the more stable (−32.11°). A constrained geometry optimization starting from the structure in the previous step was made, and the energies are plotted in Figure 4. Between 35° and 5°, substituents on the two carbons adjacent to the aminoxyl group could not be classified as either equatorial or axial, but in the step to 0°, the ring "snapped" into a conformation with the bulky substituents clearly in axial positions and the energy dropped over 0.5 kcal/mole. The calculations clearly follow two different energy minima on either side of Figure 4, with the lowest energy barrier for interconversion approximately 1.4 kcal/mol.

Three stable conformations were found for the *cis* isomer of **6**, Figure 5. The lowest energy structure has an internal hydrogen bond between the hydroperoxyl group and the carbonyl oxygen of the ester, Figure 5A. Both groups are forced into an axial position. Another stable conformation has the hydroperoxyl group hydrogen bonded to the aminoxyl oxygen, Figure 5B, and is ~0.15 kcal/mol higher in energy. The third conformation has the same hydrogen bonding as in Figure 5B, but the ester group is rotated about its bond to the pyrroline ring and lies ~0.28 kcal/mol above the structure in Figure 5A. These three minima are similar to those found for the hydroxyl radical adduct of **5**.[10]

We therefore examined the energies of *cis* **6** as the ester group was rotated. Starting from the lowest energy structure, corresponding to a dihedral angle for the ester group of 168.8°, the energy increased roughly quadratically as the ester group was rotated (Figure 6, solid

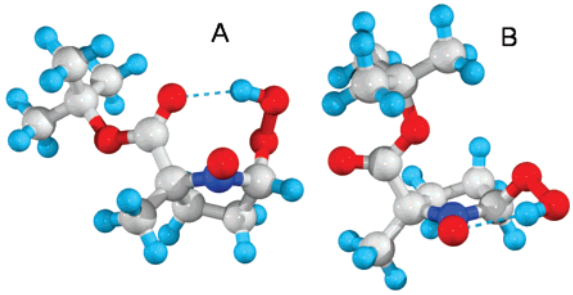

FIGURE 5. Two lowest-energy conformations of the *cis* aminoxyl **6**. (A) The lowest energy conformation with the hydrogen bond indicated by the dashed line between the hydrogen atom on the hydroperoxy group and the carbonyl oxygen of the ester; (**B**) the next most stable conformation, 0.62 kJ/mol higher in energy with the hydrogen bond indicated by the dashed line between the hydrogen atom on the hydroperoxy group and the aminoxyl oxygen.

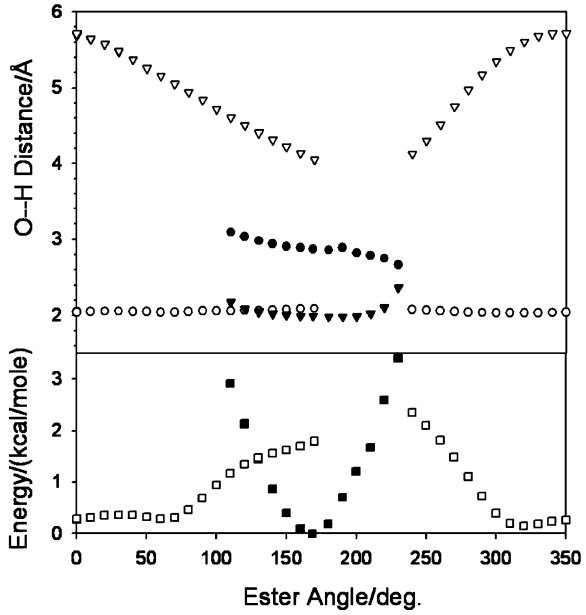

FIGURE 6. DFT energies (■, □) and H−O bond distances to the aminoxyl (●, ○) or carbonyl (▼, ▽) oxygen calculated from constrained geometry optimization as a function of the ester dihedral angle of *cis* **6**. Optimizations were done in order starting from the two lowest energy minimum to trace out the shape of the potential energy minima. The solid symbols for energy and distances belong to structures starting from that in Figure 5A, whereas the open symbols start from the structure in Figure 5B.

symbols). The length of the hydrogen bond increased from 1.987 to 2.364 Å as the energy increased by 3.40 kcal/mol.

Starting from the conformation in Figure 5B with an ester dihedral angle of ~320°, the energy varied less than 0.2 kcal/mol over a wide range with two very shallow minima. The energy increased appreciably, Figure 6, open symbols, as the carbonyl group approached an orientation where it could form a hydrogen bond. When the ester dihedral angle was the same as for the lowest energy state, the conformation with the internal hydrogen bond to the aminoxyl group was 1.6 kcal/mol higher in energy. These are two distinct sets of local minima on the potential energy surface.

(10) Villamena, F. A.; Hadad, C. M.; Zweier, J. L. *J. Am. Chem. Soc.* **2004**, 126, 1816−1829.

Figure 6 shows the local minima crossing at ~1.4 kcal/mol in vacuo at an ester dihedral angle of 130°. This represents a lower limit on the energy barrier for interconversion, because there is an additional barrier separating these local minima. An examination of the hydrogen bond distances in the upper panel of that figure indicates that these are two distinct structures at this ester dihedral angle. There are substantial differences in the distance between the hydrogen atom on the hydroperoxyl and the aminoxyl oxygen, 2.004 or 4.219 Å, and for the hydrogen atom to carbonyl oxygen distance, 2.909 or 2.073 Å. One hydrogen bond is broken and another is formed. This process and the barriers for interconversion of the structures in Figure 5 will be significantly altered in a hydrogen bonding solvent.

Conclusions

Our results find that nitrones **5a** and **5b** react with $O_2^{\bullet-}$ under our assay conditions with identical rates to give **6a** and **6b.** The products have identical EPR spectra and lifetimes in solution with the same ratio of *cis* and *trans* isomers. Quantum chemical modeling in vacuo also finds no difference, aside from the expected optical activity, arising from the difference in stereochemistry. Thus, spin trapping measurements with **5a**, **5b**, or the racemate **5** are expected to give indistinguishable results in the absence of specific interactions with proteins or other chiral biomolecules.

Experimental Section

General. Diethylenetriaminepentaacetic acid (DTPA), hypoxanthine, xanthine oxidase (EC 1.1.3.22), superoxide dismutase (SOD), and Chelex 100 ion exchange resin were purchased from commercial sources. 5-*tert*-Butoxycarbonyl-5-methyl-1-pyrroline *N*-oxide **5** was synthesized as described in the literature.[7d,e] All other chemicals were of reagent grade unless indicated otherwise.

The analytical chromatography was performed on a 4.6 mm × 25 cm 5 μ ChiralPak AD H column eluting with hexanes/ethanol/methanol/diethylamine (95:2.5:2.4:0.1) at 1.0 mL/min at 25°C. Preparative chromatography was performed using the same solvent and temperature on a 50 mm × 500 cm 20 μ ChiralPak AD H column eluting at 10.0 mL/min. Detection was by UV at 250 nm using a diode array detector.

The polarimetry experiments were conducted at a temperature of 22 °C with a cell path of 10 cm. The instrument was calibrated immediately before the rotation measurements were made, and the calibration was confirmed immediately at the conclusion of the experiments.

Generation of Superoxide. Superoxide was generated for spin trapping experiments using hypoxanthine/xanthine oxidase at pH 7.4. Typically, $O_2^{\bullet-}$ production was generated by mixing hypoxanthine (400 μM), and sufficient xanthine oxidase in sodium phosphate buffer (50 mM, Chelexed, at pH 7.0 containing 1 mM DTPA) to reach a rate of $O_2^{\bullet-}$ generation of ~1 μM/min. Control experiments contained SOD (30 U/mL).

Spin Trapping Superoxide. EPR spectra of aminoxyls **6a** and **6b**, derived from the reaction of $O_2^{\bullet-}$ with nitrones **5a** and **5b**, were recorded on an EPR spectrometer. Nitrones (50 mM) were added to each of the $O_2^{\bullet-}$ generating systems. Reaction mixtures were transferred to a flat quartz cell, fitted into the cavity of the EPR spectrometer, and spectra were recorded at room temperature. Instrumentation settings were microwave power, 20 mW; modulation frequency, 100 kHz; modulation amplitude, 0.5 G; response time, 0.5 s; and sweep, 12.5 G/min.

Modeling. The energies of different conformations and isomers of **6** in vacuo were calculated using density functional theory (DFT) methods implemented in the NWChem software suite.[11] The spin unrestricted B3LYP parametrization was used throughout with the 6-31+G* basis set for all atoms. Geometry optimizations were performed for both aminoxyls from several starting conformations in order to identify the most stable local conformations. Constrained geometry optimizations were performed as the dihedral angle of the bond between the two methylene carbons or the bond connecting the ester group to the ring was varied. At no time was there any difference in either energy or structure between the two mirror image compounds **6a** and **6b**. Frequency calculations for all the optimized structures show they are true local minima with positive frequencies. Away from those minima, there were negative frequencies as expected. The zero point corrections to the energies alter the relative stability of the minima; however, the minima remain within kT of each other at room temperature.

Acknowledgment. This work was supported in part by grants from the National Institutes of Health, EB-2034 and GM-61904. This work was performed in part at the W. R. Wiley Environmental Molecular Sciences Laboratory, a national user facility sponsored by the U.S. Department of Energy's Office of Biological and Environmental Research and located at Pacific Northwest National Laboratory, operated by Battelle for the DOE. Finally, we would like to thank Mr. James Lee of Chiral for his help in obtaining optically pure nitrones.

Supporting Information Available: Coordinates, bond angles and lengths for the four optimized structures in Figures 3 and 5. This material is available free of charge via the Internet at http://pubs.acs.org.

JO050692F

(11) (a) Straatsma, T. P.; Aprà, E.; Windus, T. L.; Bylaska, E. J.; de Jong, W.; Hirata, S.; Valiev, M.; Hackler, M. T.; Pollack, L.; Harrison, R. J.; Dupuis, M.; Smith, D. M. A.; Nieplocha, J.; Tipparaju V.; Krishnan, M.; Auer, A. A.; Brown, E.; Cisneros, G.; Fann, G. I.; Fruchtl, H.; Garza, J.; Hirao, K.; Kendall, R.; Nichols, J.; Tsemekhman, K.; Wolinski, K.; Anchell, J.; Bernholdt, D.; Borowski, P.; Clark, T.; Clerc, D.; Dachsel, H.; Deegan, M.; Dyall, K.; Elwood, D.; Glendening, E.; Gutowski, M.; Hess, A.; Jaffe, J.; Johnson, B.; Ju, J.; Kobayashi, R.; Kutteh, R.; Lin, Z.; Littlefield, R.; Long, X.; Meng, B.; Nakajima, T.; Niu, S.; Rosing, M.; Sandrone, G.; Stave, M.; Taylor, H.; Thomas, G.; van Lenthe, J.; Wong, A.; Zhang, Z. *NWChem, A Computational Chemistry Package for Parallel Computers*, Version 4.6; Pacific Northwest National Laboratory: Richland, WA 99352-0999, 2004; a modified version. (b) Kendall, R. A.; Aprà, E.; Bernholdt, D. E.; Bylaska, E. J.; Dupuis, M.; Fann, G. I.; Harrison, R. J.; Ju, J.; Nichols, J. A.; Nieplocha, J.; Straatsma, T. P.; Windus, T. L.; Wong, A. T. *Comput. Phys. Commun.* **2000**, 128, 260−283.